


Article

Performance Optimizations of the Transcritical CO₂ Two-Stage Compression Refrigeration System and Influences of the Auxiliary Gas Cooler

Yuyao Sun ^{1,2}, Jinfeng Wang ^{1,2,3,*} and Jing Xie ^{1,2,3,4,*} 

¹ College of Food Science and Technology, Shanghai Ocean University, Shanghai 201306, China; bj2012_0225@126.com

² Shanghai Professional Technology Service Platform on Cold Chain Equipment Performance and Energy Saving Evaluation, Shanghai 201306, China

³ Shanghai Engineering Research Center of Aquatic Product Processing & Preservation, Shanghai 201306, China

⁴ National Experimental Teaching Demonstration Center for Food Science and Engineering, Shanghai Ocean University, Shanghai 201306, China

* Correspondence: jfwang@shou.edu.cn (J.W.); jxie@shou.edu.cn (J.X.); Tel.: +86-156-9216-6726 (J.W.); +86-156-9216-5513 (J.X.)

Abstract: To optimize the performance of the transcritical CO₂ two-stage compression refrigeration system, the energy analysis and the exergy analysis are conducted. It is found that higher COP, lower compression power, and less exergy destruction can be achieved when the auxiliary gas cooler is applied. Moreover, the discharge temperature of the compound compressor (HPS) can be reduced by decreasing the temperature at the outlet of the auxiliary gas cooler ($T_{agc,out}$). When the $T_{agc,out}$ is reduced from 30 to 12 °C, the discharge temperature of the compound compressor (HPS) can be decreased by 13.83 °C. Furthermore, the COP and the exergy efficiency can be raised by enhancing the intermediate pressure. Based on these results, the optimizations of system design and system operation are put forward. The application of the auxiliary gas cooler can improve the performance of the transcritical CO₂ two-stage compression refrigeration system. Operators can decrease the discharge temperature of the compound compressor (HPS) by reducing the $T_{agc,out}$, and increase the COP and the exergy efficiency by enhancing the intermediate pressure.

Keywords: energy analysis; exergy analysis; coefficient of performance; exergy efficiency; auxiliary gas cooler; intermediate pressure



Citation: Sun, Y.; Wang, J.; Xie, J. Performance Optimizations of the Transcritical CO₂ Two-Stage Compression Refrigeration System and Influences of the Auxiliary Gas Cooler. *Energies* **2021**, *14*, 5578. <https://doi.org/10.3390/en14175578>

Academic Editor: Tatiana Morosuk

Received: 28 July 2021

Accepted: 3 September 2021

Published: 6 September 2021

Publisher's Note: MDPI stays neutral with regard to jurisdictional claims in published maps and institutional affiliations.



Copyright: © 2021 by the authors. Licensee MDPI, Basel, Switzerland. This article is an open access article distributed under the terms and conditions of the Creative Commons Attribution (CC BY) license (<https://creativecommons.org/licenses/by/4.0/>).

1. Instruction

Over the past decades, the greenhouse effect has appeared, and the utilization of artificial refrigerants is one of the main reasons for this [1–3]. Thus, many policies impose strict limits on the requirements for refrigerants, such as the EU F-Gas Regulation and Montreal Protocol [4–6]. To replace artificial refrigerants gradually, more and more natural refrigerants are used [7]. CO₂ is the most promising natural refrigerant whose global warming potential (GWP) and ozone depletion potential (ODP) are 1 and 0, respectively [8,9]. Besides the excellent thermophysical properties, there are some advantages of CO₂, such as being nontoxic, environmentally friendly, nonflammable, easily available, and inexpensive [10]. In terms of the CO₂ refrigerant, the critical temperature is low, and the critical pressure is high [11]. The energy efficiency of the transcritical CO₂ refrigeration cycle is higher than that of the traditional refrigeration cycles with other refrigerants, such as R134a [12]. Compared to the transcritical CO₂ one-stage compression refrigeration cycle, the transcritical CO₂ two-stage compression refrigeration cycle can reduce the discharge temperature, enhance the volumetric efficiency, and avoid the severe leaking [13].

Bellos et al. [14] examined the transcritical CO₂ one-stage compression refrigeration cycle and the transcritical CO₂ two-stage compression refrigeration cycle. For $T_c = 50\text{ }^\circ\text{C}$ and $T_e = -35\text{ }^\circ\text{C}$, the maximum COP of the transcritical CO₂ two-stage compression refrigeration cycle is 121.76% higher than that of the transcritical CO₂ one-stage compression refrigeration cycle. Moreover, the CO₂ refrigerant is also widely applied in the cascade refrigeration system. According to the research of Bellos et al. [15], the R152a/CO₂ cascade refrigeration system could obtain the maximum mean yearly COP (2.381) for $T_e = -35\text{ }^\circ\text{C}$.

Several researchers have investigated the performance of transcritical CO₂ two-stage compression refrigeration systems by energy analysis and exergy analysis. Coefficient of performance (COP) is the most important parameter in the energy analysis [16]. Exergy efficiency and exergy destruction are the main parameters in the exergy analysis [17]. Luca et al. [18] investigated five various CO₂ compression refrigeration systems when the T_e was 4, -10, and -30 °C. It was discovered that COP of the single-throttling, double-compression cycle was the best. Zhang et al. [19] researched a transcritical CO₂ refrigeration cycle including the double-compression flash intercooler. Compared to the refrigeration system without flash intercooler, the COP of the refrigeration system with a double-compression flash intercooler could be improved by 12.16%. Bruno et al. [20] studied the variable-speed CO₂ refrigeration system. When compressor speeds were 45, 60, and 75 Hz, the concentric tube internal heat exchanger could improve COP by 12.9%, 16.9%, and 17.2%, respectively. Moreover, when the flash gas bypass cycle was used, the COP could be improved, resulting in 15.5%, 18.4%, and 18.1%, respectively. Liu et al. [21] investigated the transcritical CO₂ two-stage compression refrigeration system. It was discovered that higher COP could be obtained from the transcritical CO₂ two-stage compression refrigeration system with high-pressure mechanical subcooling system. The COP of this refrigeration system could be improved by 17.47% more than that of the system without a high-pressure mechanical subcooling system. Liu et al. [22] proposed a transcritical CO₂ two-stage compression refrigeration cycle with dual evaporators and one ejector. COP and exergy efficiency of this refrigeration cycle were increased by 19.6% and 15.9% more than that of the conventional refrigeration cycle without any ejector, respectively. Paride [23] investigated the transcritical R744 supermarket refrigeration system. The improvement of utilizing overfed evaporators and parallel compressor in the transcritical CO₂ two-stage compression refrigeration system was proposed. Total irreversibilities and total unavoidable irreversibilities of two refrigeration systems were analyzed by exergy analysis. It was found that the improvement caused total irreversibilities and total unavoidable irreversibilities to decrease by 25.69 kW and 0.52 kW, respectively.

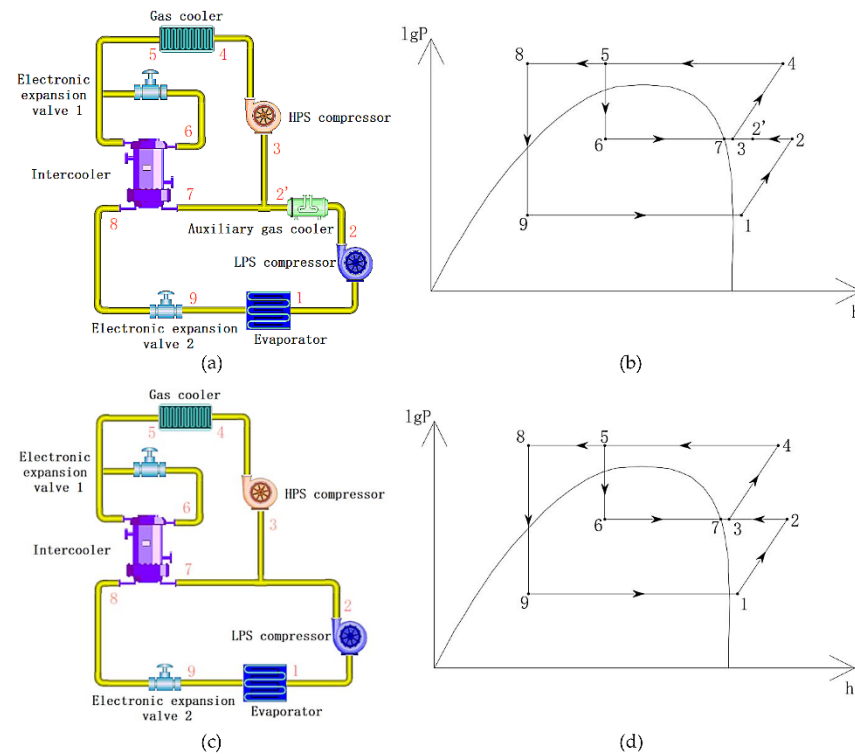
Despite rich studies on the improvement of the transcritical CO₂ two-stage compression refrigeration system, the performance impacts of the auxiliary gas cooler in the LPS and the intermediate pressure on this refrigeration system have not been investigated. In this paper, the performance comparison analysis of the transcritical CO₂ two-stage compression refrigeration system with an auxiliary gas cooler (RSF1) and the transcritical CO₂ two-stage compression refrigeration system without any auxiliary gas cooler (RSF2) is conducted; the performance impacts of intermediate pressure on the transcritical CO₂ two-stage compression refrigeration system are also investigated. The objective is to obtain the optimizations of system design and system operation for the transcritical CO₂ two-stage compression refrigeration system.

2. Descriptions of the Refrigeration System Model

The refrigeration system model studied in this paper is a transcritical CO₂ two-stage compression refrigeration system, which is used in the refrigerated container measuring $1.2 \times 1.2 \times 1.2\text{ m}$. The basic parameter values are shown in Table 1. RSF1 and RSF2 are two studied refrigeration system forms. These two forms are shown in Figure 1a,c, respectively. The pressure–enthalpy diagrams of RSF1 and RSF2 are displayed in Figure 1b,d, respectively.

Table 1. Basic parameter values of the refrigeration system.

Parameters	Value	Unit
$Q_{cooling}$	1.23	kW
T_e	−23	°C
Superheating in evaporator	3	°C
Desuperheating in gas cooler	3	°C

**Figure 1.** Transcritical CO₂ two-stage compression refrigeration system, (a) schematic (RSF1), (b) pressure–enthalpy diagram (RSF1), (c) schematic (RSF2), (d) pressure–enthalpy diagram (RSF2).

2.1. RSF1

There are eight main components used in the RSF1. These components include the LPS compressor, the HPS compressor, the auxiliary gas cooler, the gas cooler, the intercooler, the electronic expansion valve 1, the electronic expansion valve 2, and the evaporator.

In Figure 1b, all processes are as follows:

- 1→2: The compression process in the LPS compressor.
- 2→2': The gas cooling process in the auxiliary gas cooler.
- 3→4: The compression process in the HPS compressor.
- 4→5: The cooling process of the supercritical CO₂ and the desuperheating process in the gas cooler.
- 5→6: The throttling process in the electronic expansion valve 1.
- 6→7: The heat exchange process in the intercooler (the thermal energy of low-temperature CO₂ is enhanced).
- 2' + 7→3: The mixing process between high-temperature CO₂ and low-temperature CO₂.
- 5→8: The heat exchange process in the intercooler (the thermal energy of low-temperature CO₂ is decreased).
- 8→9: The throttling process in the electronic expansion valve 2.
- 9→1: The evaporation process and the superheating process in the evaporator.

2.2. RSF2

If the auxiliary gas cooler is removed, the refrigeration system will be turned to the RSF2. There are only seven main components, which are the LPS compressor, the HPS compressor, the gas cooler, the intercooler, the electronic expansion valve 1, the electronic expansion valve 2, and the evaporator.

The state point 2' is the only one canceled in Figure 1b. The process (2 + 7 → 3) becomes the mixing process between high-temperature CO₂ and low-temperature CO₂. The other processes remain unchanged.

3. Thermodynamic Model

In order to establish and simplify the thermodynamic model of the refrigeration system model, the following assumptions have been made based on the first law of thermodynamics and the second law of thermodynamics [16,24–26]:

- (1) All processes in RSF1 and RSF2 are assumed steady-state.
- (2) The reference state condition of the refrigerant is both $T_0 = 25\text{ °C}$ and $P_0 = 1\text{ atm}$ [24].
- (3) The exergy destruction in the pipes is neglected.
- (4) The kinetic effects and the potential energy effects are assumed negligible in steady flow, and there is no chemical reaction.
- (5) In all components and pipes, there is neither pressure drop, nor heat loss.
- (6) Both compression processes in the LPS compressor and the HPS compressor are adiabatic.
- (7) Both expansion processes in electronic expansion valve 1 and electronic expansion valve 2 are adiabatic and isenthalpic.
- (8) The electricity consumption of the condenser and evaporator fans is not considered.
- (9) The electrical consumption of gas cooler and auxiliary gas cooler are neglected.
- (10) All parameters are obtained from NIST 9.1 software.

3.1. Energy Analysis

Based on the first law of thermodynamics, the performance of transcritical CO₂ two-stage compression refrigeration system can be examined by COP. The formula for COP is as follows:

$$\text{COP} = \frac{Q_{cooling}}{W_{comp,tot}} \quad (1)$$

where COP is the coefficient of performance; $Q_{cooling}$ is the total cooling load, kW; $W_{comp,tot}$ is the total compression power, kW.

The $Q_{cooling}$ includes the envelope cooling load, the heat leakage cooling load, the radiant cooling load, the cooling load of equipment, and the cooling load of cargo. The detailed calculation processes for $Q_{cooling}$ have been recorded in the references [27–31].

In order to enlarge the areas for stacking chilled food, the compound compressor is chosen, which can replace the roles of both LPS compressor and HPS compressor with smaller size than using two compressors.

The formulas for $W_{comp,tot}$ are as follows:

$$q = h_1 - h_9 \quad (2)$$

$$m_{LPS} = \frac{Q_{cooling}}{q} \quad (3)$$

$$m_{HPS} = m_{LPS} \frac{h_7 - h_8}{h_7 - h_5} \quad (4)$$

$$W_{comp,LPS} = m_{LPS}(h_2 - h_1) \quad (5)$$

$$W_{comp,HPS} = m_{HPS}(h_4 - h_3) \quad (6)$$

$$W_{comp,tot} = W_{comp,LPS} + W_{comp,HPS} \quad (7)$$

where $h_1, h_2, h_3, h_4, h_5, h_7, h_8,$ and h_9 are the specific enthalpy of CO₂ at the state point 1, 2, 3, 4, 5, 7, 8, and 9, respectively, kJ/kg; m_{LPS} and m_{HPS} are the mass flow rate in the LPS and HPS, kg/s; $Q_{cooling}$ is the total cooling load, kW; q is the cooling capacity per mass, kJ/kg; $W_{comp,LPS}$ and $W_{comp,HPS}$ are the compression power of the LPS compressor and the HPS compressor, kW; $W_{comp,tot}$ is the total compression power, kW.

The isentropic efficiency of compressor is calculated by Formula (8) [16]. The values of the enthalpy of the state point 2 and the state point 4 can be calculated by Formula (9).

$$\eta_{comp} = 0.874 - 0.0135R_p \quad (8)$$

$$h_{comp,out,act} = h_{comp,in} + \frac{h_{comp,out,theo} - h_{comp,in}}{\eta_{comp}} \quad (9)$$

where $h_{comp,in}$ is the specific enthalpy of CO₂ at the inlet of the compressor, kJ/kg; $h_{comp,out,act}$ is the actual specific enthalpy of CO₂ at the outlet of the compressor, kJ/kg; $h_{comp,out,theo}$ is the theory specific enthalpy of CO₂ at the outlet of the compressor, kJ/kg; R_p is the compression ratio; η_{comp} is the isentropic efficiency.

The CO₂ from the LPS compressor and the CO₂ from the intercooler are mixed at the state point 3, so the h_3 should be acquired by the thermal balance equation. Moreover, owing to the difference between RSF1 and RSF2, the formulas of the h_3 are different. Formula (11) is used for the RSF1, and Formula (12) is used for the RSF2.

$$m_{\Delta} = m_{HPS} - m_{LPS} \quad (10)$$

$$m_{HPS} \cdot h_3 = m_{LPS} \cdot h_{2'} + m_{\Delta} \cdot h_7 \quad (11)$$

$$m_{HPS} \cdot h_3 = m_{LPS} \cdot h_2 + m_{\Delta} \cdot h_7 \quad (12)$$

where $h_2, h_{2'}, h_3,$ and h_7 are the specific enthalpy of CO₂ at the state point 2, 2', 3, and 7, respectively, kJ/kg; m_{LPS} and m_{HPS} are the mass flow rate in the LPS and HPS, kg/s; m_{Δ} is the mass flow rate difference between the LPS and HPS, kg/s.

3.2. Exergy Analysis

The exergy analysis is the method to analyze the energy conversion ability of the refrigeration system. The exergy is defined as the obtained maximum possible reversible work during the course of bringing the system into equilibrium with the environment [25]. On the basis of the second law of thermodynamics, the exergy balance equation can be expressed as follows:

$$E_{dest} = m_{in} \cdot e_{i,in} - m_{out} \cdot e_{i,out} + \left[Q_{ex} \left(1 - \frac{T_0}{T_b} \right) \right]_{in} - \left[Q_{ex} \left(1 - \frac{T_0}{T_b} \right) \right]_{out} + W_{in} - W_{out} \quad (13)$$

where E_{dest} is the exergy destruction, kW; $e_{i,in}$ and $e_{i,out}$ are the specific exergy of CO₂ at the inlet and the outlet, kJ/kg; m_{in} and m_{out} are the mass flow rate of CO₂ at the inlet and the outlet, kg/s; Q_{ex} is the heat exchange, kW; T_0 is the temperature of CO₂ at the reference state condition, K; T_b is the temperature of the heat transfer boundary, K; W_{in} and W_{out} are the inlet power and the outlet power, kW.

The e_i is the specific exergy. The formula for e_i is as follows:

$$e_i = (h_i - T_0 s_i) - (h_0 - T_0 s_0) \quad (14)$$

where e_i is the specific exergy of CO₂, kJ/kg; h_0 is the specific enthalpy of CO₂ at the reference state condition, kJ/kg; h_i is the specific enthalpy of CO₂ at the state point, kJ/kg; s_0 is the specific entropy of CO₂ at the reference state condition, kJ/(kg·K); s_i is the specific entropy of CO₂ at the state point, kJ/(kg·K); T_0 is the temperature of CO₂ at the reference state condition, K.

Besides the E_{dest} , the exergy efficiency is also an important parameter used to evaluate the energy conversion of the refrigeration system. The formula for the exergy efficiency is as follows:

$$\eta_{exergy} = 1 - \frac{E_{dest,tot}}{W_{comp}} \quad (15)$$

where η_{exergy} is the exergy efficiency; $E_{dest,tot}$ is the total exergy destruction, kW; W_{comp} is the compression power, kW.

The formulas for the compressor exergy destruction of RSF1 and RSF2 are different. The formulas are written as follows:

$$E_{dest,comp,RSF1} = E_{dest,comp,LPS} + E_{dest,comp,HPS} \quad (16)$$

$$E_{dest,comp,LPS} = m_{LPS}(e_1 - e_2) + W_{comp,LPS} \quad (17)$$

$$E_{dest,comp,HPS} = m_{HPS}(e_3 - e_4) + W_{comp,HPS} \quad (18)$$

$$E_{dest,comp,RSF2} = m_{LPS} \cdot e_1 + m_{\Delta} \cdot e_7 - m_{HPS} \cdot e_4 + W_{comp,tot} \quad (19)$$

where $E_{dest,comp,RSF1}$ and $E_{dest,comp,RSF2}$ are the compressor exergy destruction in RSF1 and RSF2, kW; $E_{dest,comp,LPS}$ and $E_{dest,comp,HPS}$ are the compressor exergy destruction in the LPS and the HPS, kW; $e_1, e_2, e_3, e_4,$ and e_7 are the specific exergy of CO₂ at the state point 1, 2, 3, 4, and 7, respectively, kJ/kg; m_{LPS} and m_{HPS} are the mass flow rate in the LPS and HPS, kg/s; $W_{comp,LPS}$ and $W_{comp,HPS}$ are the compression power of the LPS compressor and the HPS compressor, kW; $W_{comp,tot}$ is the total compression power, kW.

As for the RSF1, the exergy destruction of the auxiliary gas cooler cannot be ignored. It is necessary to calculate the compressor exergy destruction by calculating $E_{dest,comp,LPS}$ and $E_{dest,comp,HPS}$ separately, which are Formulas (16)–(18). As for the RSF2, the compressor exergy destruction should be calculated by Formula (19) [26].

The exergy destruction of the intercooler can be calculated as follows:

$$E_{dest,inter} = m_{HPS}(e_5 - e_8) + m_{\Delta}(e_6 - e_7) \quad (20)$$

where $E_{dest,inter}$ is the exergy destruction of the intercooler, kW; $e_5, e_6, e_7,$ and e_8 are the specific exergy of CO₂ at the state point 5, 6, 7, and 8, respectively, kJ/kg; m_{HPS} is the mass flow rate in the HPS, kg/s; m_{Δ} is the mass flow rate difference between the LPS and HPS, kg/s.

The exergy destruction of electronic expansion valves can be calculated as follows:

$$E_{dest,eev1} = m_{\Delta}(h_5 - h_6) \quad (21)$$

$$E_{dest,eev2} = m_{HPS}(h_8 - h_9) \quad (22)$$

where $E_{dest,eev1}$ and $E_{dest,eev2}$ are the exergy destruction of electronic expansion valve 1 and electronic expansion valve 2, kW; $h_5, h_6, h_8,$ and h_9 are the specific enthalpy of CO₂ at the state point 5, 6, 8, and 9, respectively, kJ/kg; m_{HPS} is the mass flow rate in the HPS, kg/s; m_{Δ} is the mass flow rate difference between the LPS and HPS, kg/s.

The exergy destruction of the gas cooler can be calculated as follows:

$$E_{dest,gc} = m_{HPS}(e_4 - e_5) - Q_{ex,gc} \left(1 - \frac{T_0}{T_{b,gc}} \right) \quad (23)$$

where $E_{dest,gc}$ is the exergy destruction of the gas cooler, kW; e_4 and e_5 are the specific exergy of CO₂ at the state point 4 and 5, kJ/kg; m_{HPS} is the mass flow rate in the HPS, kg/s; $Q_{ex,gc}$ is the heat exchange of gas cooler, kW; T_0 is the temperature of CO₂ at the reference state condition, K; $T_{b,gc}$ is the temperature of the heat transfer boundary of gas cooler, K.

The exergy destruction of the evaporator can be calculated as follows:

$$E_{dest, evap} = m_{LPS}(e_9 - e_1) + Q_{ex, evap} \left(1 - \frac{T_0}{T_{b, evap}} \right) \quad (24)$$

where $E_{dest, evap}$ is the exergy destruction of the evaporator, kW; e_1 and e_9 are the specific exergy of CO₂ at the state point 1 and 9, kJ/kg; m_{LPS} is the mass flow rate in the LPS, kg/s; $Q_{ex, evap}$ is the heat exchange of evaporator, kW; T_0 is the temperature of CO₂ at the reference state condition, K; $T_{b, gc}$ is the temperature of the heat transfer boundary of evaporator, K.

The exergy destruction of the auxiliary gas cooler can be calculated as follows:

$$E_{dest, agc} = m_{LPS}(e_2 - e_{2'}) - Q_{ex, agc} \left(1 - \frac{T_0}{T_{b, agc}} \right) \quad (25)$$

where $E_{dest, agc}$ is the exergy destruction of the auxiliary gas cooler, kW; e_2 and $e_{2'}$ are the specific exergy of CO₂ at the state point 2 and 2', kJ/kg; m_{LPS} is the mass flow rate in the LPS, kg/s; $Q_{ex, agc}$ is the heat exchange of auxiliary gas cooler, kW; T_0 is the temperature of CO₂ at the reference state condition, K; $T_{b, gc}$ is the temperature of the heat transfer boundary of auxiliary gas cooler, K.

In Formulas (23)–(25), T_b is the temperature of the heat transfer boundary. $T_{b, gc}$, $T_{b, evap}$, and $T_{b, ac}$ are various. The ambient temperature is chosen as the $T_{b, gc}$. The internal temperature of the refrigerated container is chosen as the $T_{b, evap}$. The intermediate temperature is chosen as the $T_{b, agc}$ [32]. The formulas for heat exchanges in each component are written as follows:

$$Q_{ex, agc} = m_{LPS}(h_2 - h_{2'}) \quad (26)$$

$$Q_{ex, gc} = m_{HPS}(h_4 - h_5) \quad (27)$$

$$Q_{ex, evap} = m_{LPS}(h_1 - h_9) \quad (28)$$

where $Q_{ex, agc}$, $Q_{ex, gc}$, and $Q_{ex, evap}$ are the heat exchange of auxiliary gas cooler, gas cooler, and evaporator, respectively, kW; h_1 , h_2 , $h_{2'}$, h_4 , h_5 , and h_9 are the specific enthalpy of CO₂ at the state point 1, 2, 2', 4, 5, and 9, respectively, kJ/kg; m_{LPS} and m_{HPS} are the mass flow rate in the LPS and HPS, kg/s.

4. Results and Discussion

4.1. Performance Impacts of Different $T_{gc, out}$ and $P_{gc, out}$ on Transcritical CO₂ Two-Stage Compression Refrigeration Systems

In the recent research, the effect of different T_e on various refrigeration systems is the research focus, but the research about T_c is few, especially in the transcritical CO₂ two-stage compression refrigeration system. With regards to RSF1 and RSF2, the T_e is -23 °C. The effects of both different $T_{gc, out}$ and $P_{gc, out}$ on RSF1 and RSF2 is one of the research contents.

In the initial study, five selected $T_{gc, outs}$ are 33, 35, 37, 39, and 41 °C; five selected $P_{gc, outs}$ are 8.9, 9.1, 9.3, 9.5, and 9.7 MPa. The variation of COP in RSF1 and RSF2 are shown in Figures 2a and 3a, respectively. COP declines with the increase of $T_{gc, out}$. Three trends of COP can be divided with the increasing $P_{gc, out}$:

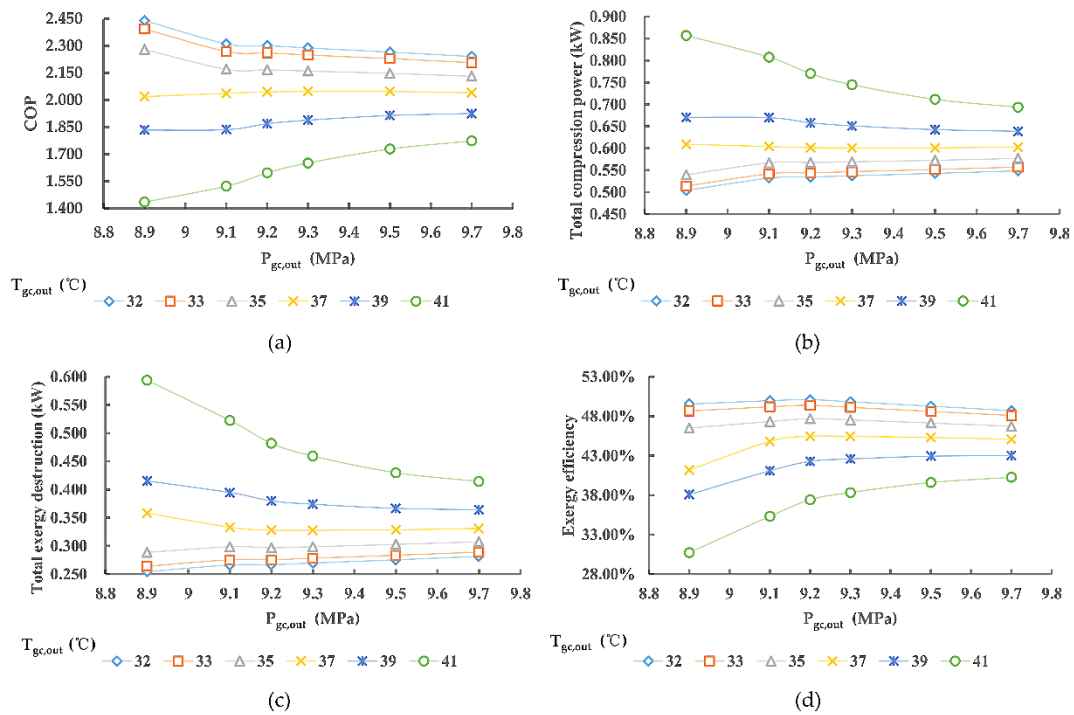


Figure 2. Performance of the RSF1 with various $P_{gc,out}$ and $T_{gc,out}$, (a) COP, (b) total compression power, (c) total exergy destruction, (d) exergy efficiency.

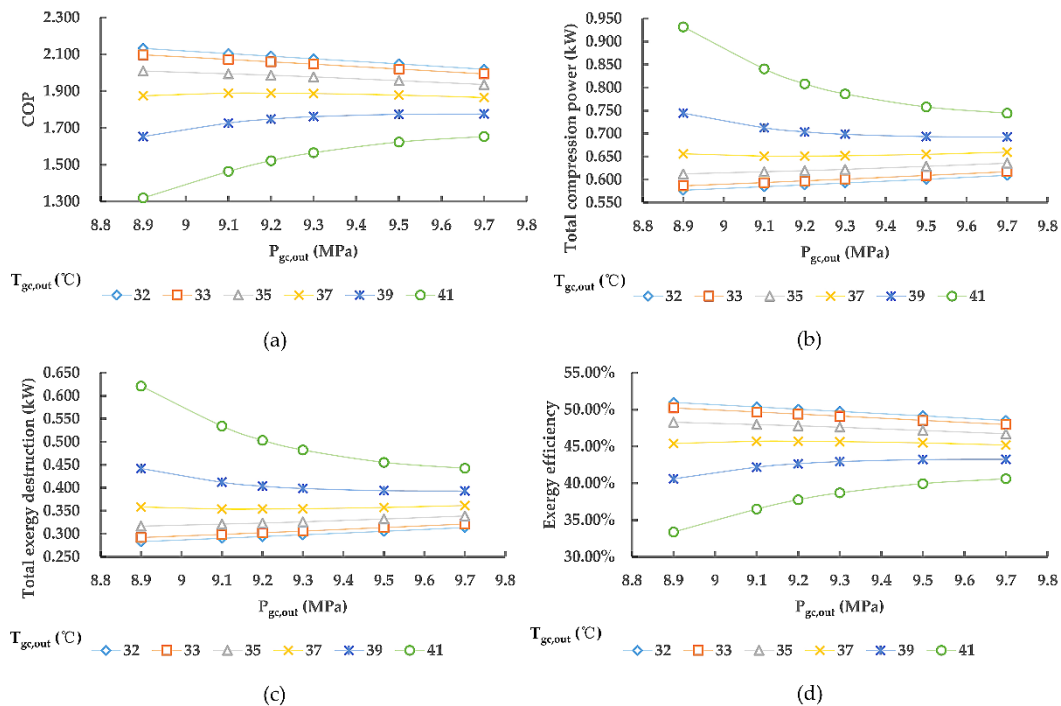


Figure 3. Performance of the RF2 with various $P_{gc,out}$ and $T_{gc,out}$, (a) COP, (b) total compression power, (c) total exergy destruction, (d) exergy efficiency.

- (1) The COP enhances with the decrease of $P_{gc,out}$ (33 and 35 °C).
- (2) The COP raises first, then decreases with the increase of $P_{gc,out}$ (37 °C).
- (3) The COP increases with the increase of $P_{gc,out}$ (39 and 41 °C).

Based on Formula (1), the reason for this phenomenon is the change of the total compression power. The mass flow rates in each pipe change with the variation of $T_{gc,out}$

and $P_{gc,out}$, which can impact the total compression power. When the total cooling load is fixed at 1.23 kW, if the total compression power is smaller, the COP is larger. As shown in Figures 2b and 3b, the total compression power in RSF1 and RSF2 has a matching trend with Figures 2a and 3a, respectively.

According to the trend of COP, when the $P_{gc,out}$ is less than 37 °C, the value of COP is larger. In this range, to decrease both $T_{gc,out}$ and $P_{gc,out}$ can enhance the value of COP. However, the range of $T_{gc,out}$ and $P_{gc,out}$ is limited because the CO₂ is in the transcritical condition; $T_{gc,out}$ and $P_{gc,out}$ cannot be dropped below 31.1 °C and 7.38 MPa, which are critical temperature and critical pressure [33].

The total exergy destruction in RSF1 and RSF2 are shown in Figures 2c and 3c, respectively. The total exergy destruction increases with the increase of $T_{gc,out}$. When the $T_{gc,out}$ is 33 and 35 °C, the total exergy destruction decreases with the increase of $P_{gc,out}$. However, the total exergy destruction increases with the increase of $P_{gc,out}$ when the $T_{gc,out}$ is 39 and 41 °C. If the $T_{gc,out}$ is 37 °C, the total exergy destruction decreases first, then increases.

The change of $P_{gc,out}$ can influence parameters of CO₂ at the state point 2', 3, 4, 5, 6, 7, and 8. Both enthalpies and entropies are impacted. The variation trends of total compression power and total exergy destruction are similar, so it is hard to analyze by only these two parameters. The exergy efficiency can be calculated by Formula (15), which can be used to analyze the energy conversion ability of refrigeration systems clearly. The exergy efficiency of RSF1 and RSF2 is showed in Figures 2d and 3d, respectively. With the increase of $T_{gc,out}$, the exergy efficiency in RSF1 and RSF2 decreases. However, when the $P_{gc,out}$ increases, the trends of them are different. As for the RSF1, there is a maximum exergy efficiency when $T_{gc,out}$ is 33, 35, and 37 °C, which are 49.97%, 49.18%, and 47.52%, respectively. When $T_{gc,out}$ is 39 and 41 °C, the exergy efficiency enhances with the increase of $P_{gc,out}$. As for the RSF2, the exergy efficiency decreases with the increase of $P_{gc,out}$ in all $T_{gc,out}$. The higher exergy efficiency means the energy conversion ability of the refrigeration system is better [34]. Combining both COP and exergy efficiency, it is possible to find out the best operation condition of the refrigeration systems. The best operation conditions of RSF1 and RSF2 with design accuracy (temperature accuracy to the single digit, pressure accurate to the first decimal point) are as follows:

(1) The optimal operation condition of the RSF1

In terms of COP, lower $T_{gc,out}$ should be selected, but it cannot be dropped below 31.1 °C, so the $T_{gc,out}$ is identified as 32 °C. According to the abovementioned analysis, the maximum exergy efficiency occurs at $P_{gc,out} = 9.1$ or 9.3 MPa, so it is necessary to calculate the parameters when the $P_{gc,out}$ is 9.2 MPa.

As shown in Figure 2a,d, the trends of COP and exergy efficiency when the $T_{gc,out}$ is 32 °C are the same as those when the $T_{gc,out}$ s are 33 and 35 °C. When the $T_{gc,out}$ is 32 °C, COP increases with the decrease of $P_{gc,out}$. The largest exergy efficiency (50.10%) occurs when the $P_{gc,out}$ is 9.2 MPa.

Based on the energy saving requirements, the energy conversion ability is the main selection standard, so the optimal operation condition of RSF1 is obtained at both $T_{gc,out} = 32$ °C and $P_{gc,out} = 9.2$ MPa ($\eta_{exergy} = 50.10\%$, COP = 2.301).

(2) The optimal operation condition of the RSF2

Based on the variation of RSF1, a conjecture is put forward that the maximum exergy efficiency still exists in the RSF2, but the range of the extreme point changes. It is observable from Table 2 that when the $P_{gc,out}$ is 8.0 MPa, the exergy efficiency (53.15%) is maximum. Therefore, the optimal operation condition of RSF2 is obtained at both $T_{gc,out} = 32$ °C and $P_{gc,out} = 8.0$ MPa ($\eta_{exergy} = 53.15\%$, COP = 2.233).

Table 2. Parameter values studied in the RSF2 when the $T_{gc,out}$ is 32 °C.

$P_{gc,out}$ (MPa)	COP	Exergy Efficiency	Total Exergy Destruction (kW)	Total Compression Power (kW)
7.4	1.275	32.39%	0.652	0.965
7.7	2.215	52.75%	0.262	0.555
7.9	2.232	53.13%	0.2582	0.5510
8.0	2.233	53.15%	0.2580	0.5508
8.1	2.227	53.02%	0.259	0.552
8.3	2.205	52.55%	0.265	0.558
8.6	2.167	51.72%	0.274	0.568

The model can be validated by the data from reference [14]. As shown in Table 3, for $T_{gc,out} = 35$ °C, $T_e = -23$ °C, and $P_{gc,out} = 9.1$ MPa, the values of COP of RSF2 and the refrigeration system in reference [14] are 1.986 and 1.959, respectively. The deviation is 1.38% which is acceptable. Moreover, in terms of the refrigeration system in [14], if the T_e and the $P_{gc,out}$ are fixed, the COP increases with the decrease of $T_{gc,out}$. This trend is the same as that of RSF2.

Table 3. Values of COP of RSF2 and reference [14] for $T_{gc,out} = 35$ °C, $T_e = -23$ °C and $P_{gc,out} = 9.1$ MPa.

Parameter	RSF2	Reference [14]	Deviation (%)
COP	1.986	1.959	1.38%

4.2. Performance Impacts of the Auxiliary Gas Cooler on Transcritical CO₂ Two-Stage Compression Refrigeration Systems

As for traditional transcritical CO₂ two-stage compression refrigeration systems, the auxiliary gas cooler is not in use. In this research, the impact of the auxiliary gas cooler on the transcritical CO₂ two-stage compression refrigeration system is studied.

The variation trends of COP, exergy efficiency, total exergy destruction, and total compression power in RSF1 and RSF2 are shown in Figures 2 and 3. The variation trends of COP, total exergy destruction, and total compression power are similar in RSF1 and RSF2. In the same operation conditions, it is discovered that higher COP, lower total compression power, and less exergy destruction can be obtained in the RSF1.

The temperature of 32 °C is the $T_{gc,out}$ of the optimal operation condition of RSF1 and RSF2, but the $P_{gc,out}$ s of the optimal operation conditions in RSF1 and RSF2 are different. As for RSF1, the maximum exergy efficiency appears when the $P_{gc,out}$ is 9.2 MPa. As for RSF2, the maximum exergy efficiency appears when the $P_{gc,out}$ is 8.0 MPa. Viewing the difference of exergy efficiency and COP between the best operation conditions of RSF1 and RSF2, the exergy efficiency of RSF2 is 3.05% higher than that of RSF1, but the COP of RSF2 is 0.068 lower than that of RSF1.

As for the RSF1, the design standard ($T_3 = T_7 + 5$ °C) [35] can be obeyed by adjusting the auxiliary gas cooler. However, the CO₂ of the state point 3 depends on the natural mix between the CO₂ of state points 2 and 7 in the RSF2. Figure 4 describes the temperature difference between T_3 and T_7 (TD3–7) in the RSF2. It is noticed that TD3–7 increases with the increase of $P_{gc,out}$ and decreases with the increase of $T_{gc,out}$. Furthermore, the minimum TD3–7 is 8.29 °C which is still higher than the design required TD3–7. The maximum TD3–7 is 23.10 °C. Based on Formula (9), the higher the T_3 is, the higher the discharge temperature of the compound compressor (HPS) will be. Higher discharge temperature can cause higher possibility of lubricant oil carbonization in the compressor [36]. The application of auxiliary gas cooler can conquer this problem well.

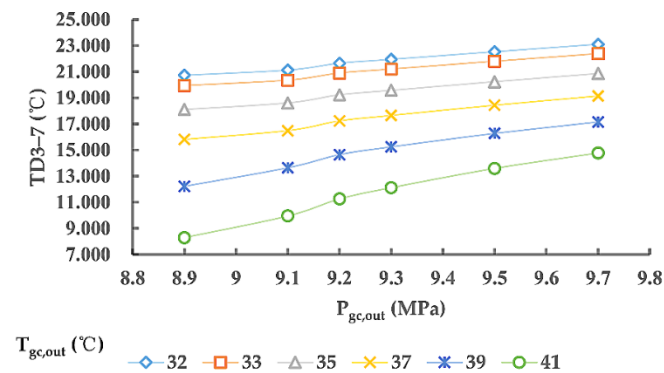


Figure 4. Temperature difference between T_3 and T_7 in the RSF2.

T_4 is the discharge temperature of the compound compressor (HPS). Figure 5a describes the trend of T_4 in RSF1. When the $P_{gc,out}$ is fixed, T_4 is also fixed, but when the $T_{gc,out}$ is fixed, T_4 enhances with the increase of $P_{gc,out}$. Figure 5b describes the trend of T_4 in RSF2. When the $T_{gc,out}$ is fixed, T_4 enhances with the increase of $P_{gc,out}$. When the $P_{gc,out}$ is fixed, T_4 decreases with the increase of $T_{gc,out}$. Moreover, T_4 is much larger in RSF2. The maximum T_4 of RSF2 is 104.48 °C, while the maximum T_4 of RSF1 is 81.44 °C, and the difference between them is up to 23.04 °C. Lower the discharge temperature can decrease the possibility of the lubricant oil carbonization in the compressor, which can ensure the compressor is well lubricated for a long time and improve the reliability of the refrigeration system [36]. Therefore, the utilization of the auxiliary gas cooler is beneficial to reduce T_4 .

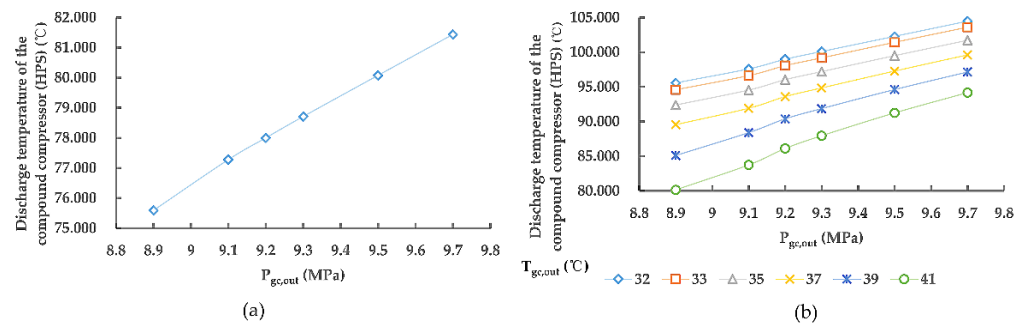


Figure 5. Discharge temperature of the compound compressor (HPS), (a) RSF1, (b) RSF2.

The variation of the performance of RSF1 with different $T_{agc,out}$ is also necessary to study. The $T_{agc,out}$ in the optimal operation condition is 13.88 °C, so there are five temperatures chosen as the initial studied $T_{agc,out}$, which are 12, 13, 14, 15, and 16 °C. As shown in Figure 6, the COP decreases with the increase of $T_{agc,out}$, but exergy efficiency increases with the increase of $T_{agc,out}$. The trends of COP and exergy efficiency are opposite. When the $T_{agc,out}$ changes from 12 to 16 °C, COP changes by 0.039 (from 2.320 to 2.281) and exergy efficiency changes by 0.04% (from 50.08% to 50.12%). Moreover, based on the above studies, the $T_{agc,out} = 20, 25,$ and 30 °C are also studied. The values of COP and exergy efficiency with $T_{agc,out} = 20, 25,$ and 30 °C are shown in Table 4. When the $T_{agc,out}$ changes from 16 to 20 °C, COP changes by 0.038 and exergy efficiency changes by 0.08%. When the $T_{agc,out}$ changes from 20 to 25 °C, COP changes by 0.041 and exergy efficiency changes by 0.13%. When the $T_{agc,out}$ changes from 25 to 30 °C, COP changes by 0.037 and exergy efficiency changes by 0.15%. It is noted that $T_{agc,out}$ has a small effect on COP and exergy efficiency. Based on Formulas (9) and (11), higher $T_{agc,out}$ can increase the discharge temperature of the compound compressor (HPS), which will cause higher possibility of the lubricant oil carbonization in the compressor [36]. The $T_{agc,out}$ is usually determined according to design requirements. Moreover, the discharge temperature of the compound compressor (HPS) can be declined by decreasing $T_{agc,out}$. For $T_{agc,out} = 12$

and 30 °C, the discharge temperatures of the compound compressor (HPS) are 76.45 and 90.28 °C, respectively. The temperature difference is 13.83 °C.

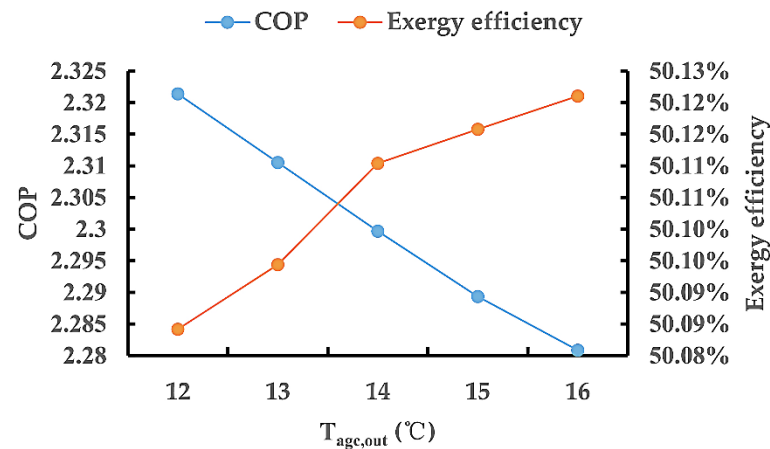


Figure 6. The influence on the RSF1 with different $T_{agc,out}$.

Table 4. COP and exergy efficiency of the RSF1 with different $T_{agc,out}$.

$T_{agc,out}$	COP	Exergy Efficiency
20	2.243	50.20%
25	2.202	50.33%
30	2.165	50.48%

4.3. Performance Optimization of the Transcritical CO₂ Two-Stage Compression Refrigeration System during Ambient Temperature Changes

Many refrigerated containers are used in maritime transportation. In different maritime areas, ambient temperatures are various. The maximum ambient temperatures of different maritime areas are shown in Table 5. The T_c equals the sum of $T_{gc,out}$ and supercooling, which should be higher than the ambient temperature. If refrigerated containers need to be transported across several maritime areas, the T_c must meet the requirement of the highest ambient temperature. However, the performance of the refrigeration system may not be the best in this situation. It is inconvenient to adjust the gas cooler one by one when the ambient temperature changes. In this paper, a method is proposed to solve the problem by adjusting the intermediate pressure.

Table 5. Maximum ambient temperatures of different maritime areas.

Maritime Areas/Design Parameter	Maximum Ambient Temperature	Sources of the Data
Design parameter	40 °C	Reference [27]
Bohai Sea	32 °C	Standard Q/HS 3008-2016
East China Sea	32 °C	Standard Q/HS 3008-2016
Yellow Sea	32 °C	Standard Q/HS 3008-2016
South China Sea	35 °C	Standard Q/HS 3008-2016
Northwest Pacific Ocean	33.44 °C	Official website of ECMWF
South Atlantic Ocean	31.15 °C	Official website of ECMWF
Northwest Atlantic Ocean	30.93 °C	Official website of ECMWF
Indian Ocean	32.50 °C	Official website of ECMWF

The RSF1 is the investigated refrigeration system. The $P_{gc,out}$ is assumed as 9.2 MPa. The intermediate pressure equals the geometric mean of the condensation pressure and the evaporation pressure. When the $P_{gc,out}$ is 9.2 MPa, the intermediate pressure is 4.062 MPa.

Consequently, there are six pressures chosen as the studied intermediate pressures, which are 3.9, 4.0, 4.1, 4.2, 4.3, and 4.4 MPa.

As shown in Figure 7a, when the $T_{gc,out}$ is fixed at 32 °C, COP enhances with the increase of intermediate pressure. As shown in Figure 7b, when the $T_{gc,out}$ is fixed at 32 °C, the exergy efficiency enhances with the increase of intermediate pressure. It can be noted that if the intermediate pressure increases, the performance of the refrigeration system will be raised.

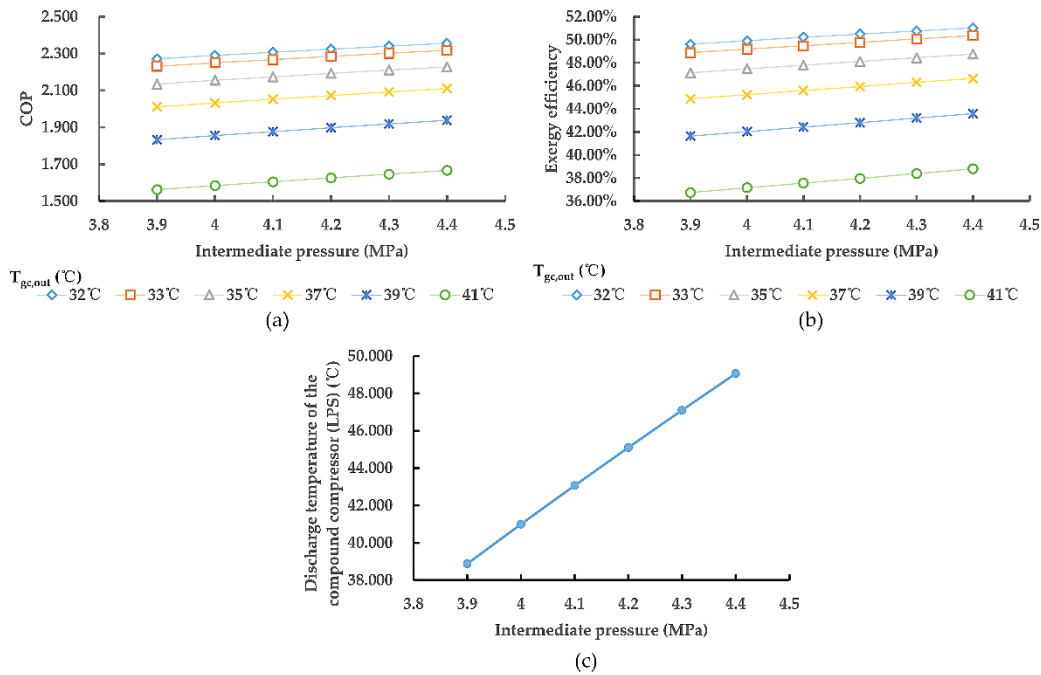


Figure 7. The influence of the adjustment of the intermediate pressure on the RSF1: (a) COP, (b) exergy efficiency, (c) discharge temperature of the compound compressor (LPS).

The curves in Figure 7a are fitted as Function (29). The growth rates of COP can be seen in Table 6, which are 0.1679, 0.1740, 0.1865, 0.1990, 0.2098, and 0.2089.

Table 6. Growth rate of COP and exergy efficiency in different $T_{gc,out}$.

$T_{gc,out}$ (°C)	Growth Rate of COP [a_1]	Growth Rate of Exergy Efficiency [a_2]
32	0.1679	2.84%
33	0.1740	2.95%
35	0.1865	3.25%
37	0.1990	3.56%
39	0.2098	3.90%
41	0.2089	4.09%

It is noted that when the $T_{gc,out}$ increases, the growth rate of COP is raised, except that the growth rate of $COP_{41^\circ C}$ is lower than that of $COP_{39^\circ C}$. However, the difference between $COP_{41^\circ C}$ and $COP_{39^\circ C}$ is only 0.0003, which can be ignored. The curves in Figure 7b are fitted as Function (30). The growth rates of exergy efficiency can be seen in Table 6 which are 2.84%, 2.95%, 3.25%, 3.56%, 3.90%, and 4.09%. When the $T_{gc,out}$ increases, the growth rate of exergy efficiency is raised. When the $P_{gc,out}$ is fixed at 9.2 MPa, both COP and exergy efficiency decrease with the increase of $T_{gc,out}$. In the operation conditions with fixed $P_{gc,out}$

and higher $T_{gc,out}$, to enhance the intermediate pressure can cause larger values of both COP and exergy efficiency.

$$\text{COP} = a_1 P_{intermediate} + b_1 \quad (29)$$

$$\eta_{exergy} = a_2 P_{intermediate} + b_2 \quad (30)$$

where COP is the coefficient of performance; $P_{intermediate}$ is the intermediate pressure, MPa; η_{exergy} is the exergy efficiency; a_1 and a_2 are the growth rate of COP and exergy efficiency, MPa^{-1} ; b_1 and b_2 are constants.

T_2 is the discharge temperature of the compound compressor (LPS). From Figure 7c, we can see that T_2 increases with the increase of intermediate pressure. The curves in Figure 7c are fitted as functions (Function (31)). If the intermediate pressure enhances 0.1 MPa, T_2 will raise 2.04 °C. Higher discharge temperature can cause higher possibility of the lubricant oil carbonization in the compressor [36]. To ensure the compressor being well lubricated for a long time and improve the reliability of the refrigeration system, the adjustment range of intermediate pressure should take the lubricant oil into account.

$$T_2 = 20.357 P_{intermediate} - 40.446 \quad (31)$$

where T_2 is the discharge temperature of the compound compressor (LPS), °C; $P_{intermediate}$ is the intermediate pressure, MPa; the unit of 20.357 is °C/MPa; the unit of 40.446 is °C.

5. Conclusions

Based on the first law of thermodynamics and the second law of thermodynamics, the thermodynamic model of the transcritical CO₂ two-stage compression refrigeration system is established. Based on energy analysis and exergy analysis, the optimizations of system design and system operation are put forward. From the above analysis, detailed conclusions can be drawn as below:

(1) For the RSF1 with $T_e = -23$ °C, the optimal operation condition of RSF1 is obtained at both $T_{gc,out} = 32$ °C and $P_{gc,out} = 9.2$ MPa. The exergy efficiency and the COP of the optimal operation condition of RSF1 are 50.10% and 2.301, respectively. For the RSF2 with $T_e = -23$ °C, the optimal operation condition of RSF2 is obtained at both $T_{gc,out} = 32$ °C and $P_{gc,out} = 8.0$ MPa. The exergy efficiency and the COP of the optimal operation condition of RSF2 are 53.15% and 2.233, respectively.

(2) In terms of the optimal operation conditions of RSF1 and RSF2, the exergy efficiency of the RSF2 is 3.05% higher than that of RSF1, but the COP of RSF2 is 0.068 lower than that of RSF1. Furthermore, in the same operation conditions, higher COP, lower compression power, and less exergy destruction can be achieved in the RSF1. Therefore, it is necessary to use the auxiliary gas cooler in the transcritical CO₂ two-stage compression refrigeration system.

(3) The COP decreases with the increase of $T_{agc,out}$, but the exergy efficiency increases with the increase of $T_{agc,out}$. The difference between COP_{12 °C} and COP_{30 °C} is 0.155. The difference between $\eta_{exergy,12 °C}$ and $\eta_{exergy,30 °C}$ is 0.4%, which is minimal. Moreover, the discharge temperature of the compound compressor (HPS) can be decreased with the decrease of $T_{agc,out}$. When $T_{agc,out}$ is reduced from 30 to 12 °C, the discharge temperature of the compound compressor (HPS) can be decreased by 13.83 °C. In the RSF1, the adjustment of $T_{agc,out}$ can be used to control the discharge temperature of the compound compressor (HPS). Operators can reduce the discharge temperature of the compound compressor (HPS) by decreasing the $T_{agc,out}$.

(4) For the RSF1 with $T_e = -23$ °C and $T_{gc,out} = 32, 33, 35, 37, 39$ and 41 °C, both COP and exergy efficiency can enhance with the increase of intermediate pressure from 3.9 MPa to 4.4 MPa. For each 0.1 MPa increase in intermediate pressure, the COPs rise 0.1679, 0.1740, 0.1865, 0.1990, 0.2098, and 0.2089 when the $T_{gc,out}$ is 32, 33, 35, 37, 39, and 41 °C, respectively. For each 0.1 MPa increase in intermediate pressure, the values of exergy efficiency rise 2.84%, 2.95%, 3.25%, 3.56%, 3.90%, and 4.09% when the $T_{gc,out}$ is 32, 33, 35, 37, 39, and 41 °C, respectively. The adjustment of the intermediate pressure is important

to control the performance of the transcritical CO₂ two-stage compression refrigeration system. Operators can increase the COP and the exergy efficiency by enhancing the intermediate pressure.

Author Contributions: Writing—original draft preparation, Y.S.; calculation and data curation, J.W.; writing—review and editing, J.X. All authors have read and agreed to the published version of the manuscript.

Funding: This research was supported by Science and Technology Innovation Action Plan of Shanghai Science and Technology Commission (19DZ1207503), Public Service Platform Project of Shanghai Science and Technology Commission (20DZ2292200).

Conflicts of Interest: The authors declare no conflict of interest.

Nomenclature

COP	coefficient of performance
E_{dest}	exergy destruction (kW)
e	specific exergy (kJ/kg)
h	specific enthalpy (kJ/kg)
m	mass flow rate (kg/s)
P	pressure (atm, MPa)
$P_{gc,out}$	pressure at the outlet of gas cooler
$Q_{cooling}$	total cooling load (kW)
Q_{ex}	heat exchange (kW)
q	cooling capacity per mass (kJ/kg)
R_p	compression ratio
RSF1	transcritical CO ₂ two-stage compression refrigeration system with an auxiliary gas cooler
RSF2	transcritical CO ₂ two-stage compression refrigeration system without any auxiliary gas cooler
s	specific entropy (kJ/(kg·K))
T	temperature (°C, K)
$T_{agc,out}$	temperature at the outlet of auxiliary gas cooler
T_c	condensation temperature (°C)
T_e	evaporation temperature (°C)
$T_{gc,out}$	temperature at the outlet of gas cooler
W_{comp}	compression power (kW)
W	power (kW)
η_{comp}	isentropic efficiency of compressor
η_{exergy}	exergy efficiency
Subscripts	
1, 2, 2', 3, 4, 5, 6, 7, 8, 9	state point
0	reference state condition
act	actual
agc	auxiliary gas cooler
b	boundary
eev1	electronic expansion valve 1
eev2	electronic expansion valve 2
evap	evaporator
gc	gas cooler
HPS	high-pressure stage
i	any state point
in	Inlet
inter	intercooler
LPS	low-pressure stage

out	outlet
theo	theory
tot	total
Δ	difference

References

- Ehsan, G.; Pedram, H.; Pouria, A. Advanced exergy analysis of a carbon dioxide ammonia cascade refrigeration system. *Appl. Therm. Eng.* **2018**, *137*, 689–699.
- Sebastian, E.; Fabian, D.; Johannes, K.; Christoph, W.; Hartmut, S. Experimental investigation of modern ORC working fluids R1224yd(Z) and R1233zd(E) as replacements for R245fa. *Appl. Energy* **2019**, *240*, 946–963.
- Kashif, N.; Ally, M.R. Options for low-global-warming-potential and natural refrigerants Part 2: Performance of refrigerants and systemic irreversibilities. *Int. J. Refrig.* **2019**, *106*, 213–224.
- Skacanová, K.Z.; Battesti, M. Global market and policy trends for CO₂ in refrigeration. *Int. J. Refrig.* **2019**, *107*, 98–104. [[CrossRef](#)]
- Gabriele, R. Molecular simulation studies on refrigerants past-present-future. *Fluid Phase Equilibria* **2019**, *485*, 190–198.
- Heath, E.A. Amendment to the Montreal protocol on substances that deplete the ozone layer (Kigali amendment). *Int. Leg. Mater.* **2017**, *56*, 193–205. [[CrossRef](#)]
- Mehdi, A.; Behzad, N.; Ali, S.; Fabio, R. Exergetic, economic and environmental (3E) analyses, and multi-objective optimization of a CO₂/NH₃ cascade refrigeration system. *Appl. Therm. Eng.* **2014**, *65*, 42–50.
- Gullo, P.; Hafner, A.; Banasiak, K. Thermodynamic Performance Investigation of Commercial R744 Booster Refrigeration Plants Based on Advanced Exergy Analysis. *Energies* **2019**, *12*, 354. [[CrossRef](#)]
- Gullo, P. Advanced Thermodynamic Analysis of a Transcritical R744 Booster Refrigerating Unit with Dedicated Mechanical Subcooling. *Energies* **2018**, *11*, 3058. [[CrossRef](#)]
- Hosseini, G.; Ighball, B.A. The application of thermoelectric and ejector in a CO₂ direct-expansion ground source heat pump; energy and exergy analysis. *Energy Convers. Manag.* **2020**, *226*, 113526.
- Bai, T.; Yu, J.L.; Yan, G. Advanced exergy analyses of an ejector expansion transcritical CO₂ refrigeration system. *Energy Convers. Manag.* **2016**, *126*, 850–861. [[CrossRef](#)]
- Song, Y.L.; Wang, H.D.; Yin, X.; Cao, F. Review of Transcritical CO₂ Vapor Compression Technology in Refrigeration and Heat Pump. *J. Refrig.* **2021**, *42*, 1–24.
- Wang, H.L.; Ma, Y.T.; Tian, J.R.; Li, M.X. Theoretical analysis and experimental research on transcritical CO₂ two stage compression cycle with two gas coolers (TSCC+TG) and the cycle with intercooler (TSCC+IC). *Energy Convers. Manag.* **2011**, *52*, 2819–2828. [[CrossRef](#)]
- Bellos, E.; Tzivanidis, C. A comparative study of CO₂ refrigeration systems. *Energy Convers. Manag. X* **2019**, *X 1*, 100002. [[CrossRef](#)]
- Bellos, E.; Tzivanidis, C. A Theoretical Comparative Study of CO₂ Cascade Refrigeration Systems. *Appl. Sci.* **2019**, *9*, 790. [[CrossRef](#)]
- Yan, G.; Hu, H.; Yu, J.L. Performance evaluation on an internal auto-cascade refrigeration cycle with mixture refrigerant R290/R600a. *Appl. Therm. Eng.* **2015**, *75*, 994–1000. [[CrossRef](#)]
- Ali, L.T.; Mushtaq, T.H.; Wasan, A.J. Thermal and exergy analysis of optimal performance and refrigerant for an air conditioner split unit under different Iraq climatic conditions. *Therm. Sci. Eng. Prog.* **2020**, *19*, 100595.
- Luca, C.; Manuel, C.; Marco, C.; Ezio, F.; Silvia, M.; Paolo, S.; Claudio, Z. Thermodynamic analysis of different two-stage transcritical carbon dioxide cycles. *Int. J. Refrig.* **2009**, *32*, 1058–1067.
- Zhang, Z.Y.; Wang, H.L.; Tian, L.L.; Huang, C.S. Thermodynamic analysis of double-compression flash intercooling transcritical CO₂ refrigeration cycle. *J. Supercrit. Fluids* **2016**, *109*, 100–108. [[CrossRef](#)]
- Bruno, Y.K.D.C.; Cláudio, M.; Roberto, H.P. An experimental study on the use of variable capacity two-stage compressors in transcritical carbon dioxide light commercial refrigerating systems. *Int. J. Refrig.* **2019**, *106*, 604–615.
- Liu, S.C.; Lu, F.P.; Dai, B.M.; Victor, N.; Li, H.L.; Qi, H.F.; Li, J.Y. Performance analysis of two-stage compression transcritical CO₂ refrigeration system with R290 mechanical subcooling unit. *Energy* **2019**, *189*, 116143. [[CrossRef](#)]
- Liu, Y.; Liu, J.R.; Yu, J.L. Theoretical analysis on a novel two-stage compression transcritical CO₂ dual-evaporator refrigeration cycle with an ejector. *Int. J. Refrig.* **2020**, *119*, 268–275. [[CrossRef](#)]
- Paride, G. Impact and quantification of various individual thermodynamic improvements for transcritical R744 supermarket refrigeration systems based on advanced exergy analysis. *Energy Convers. Manag.* **2021**, *229*, 113684.
- Zhang, Y.; Liang, T.Y.; Yang, C.; Zhang, X.L.; Yang, K. Advanced exergy analysis of an integrated energy storage system based on transcritical CO₂ energy storage and Organic Rankine Cycle. *Energy Convers. Manag.* **2020**, *216*, 112938. [[CrossRef](#)]
- Kumar, R. Computational energy and exergy analysis of R134a, R1234yf, R1234ze and their mixtures in vapour compression system. *Ain Shams Eng. J.* **2018**, *9*, 3229–3237.
- Sun, J.; Li, W.H.; Cui, B.R. Energy and exergy analyses of R513a as a R134a drop-in replacement in a vapor compression refrigeration system. *Int. J. Refrig.* **2020**, *112*, 348–356. [[CrossRef](#)]
- Xue, W. The Design of a Refrigeration Unit for Marine Reefer Container and its Performance Research. Master's Thesis, Jimei University, Xiamen, China, 2013.

28. Li, M.C. Performance of the Radiant Cooling System on the Roof of LNG-fueled Refrigerated Vehicles. Master's Thesis, Zhongyuan University of Technology, Zhengzhou, China, 2019.
29. Han, F.F. Simulation research on the cold storage LNG refrigerated truck with multi-temperature zone. Master's Thesis, North China Electric Power University, Beijing, China, 2018.
30. Zhao, X.X. Multi-temperature Distribution Optimization and Precise Temperature Regulation of Refrigerated Truck. Master's Thesis, Shandong University, Jinan, China, 2014.
31. Guo, Y.G. Research on Temperature Field Distribution of Cold Plate Refrigerated Truck and Effects on Preservation of Vegetables. Master's Thesis, Tianjin University of Commerce, Tianjin, China, 2014.
32. Sivakumar, M.; Somasundaram, P. Exergy and energy analysis of three stage auto refrigerating cascade system using Zeotropic mixture for sustainable development. *Energy Convers. Manag.* **2014**, *84*, 589–596. [[CrossRef](#)]
33. Chen, Y.; Xu, D.J.; Chen, Z.; Gao, X.; Ren, F.K.; Han, W. Performance Analysis and Evaluation of a Supercritical CO₂ Rankine Cycle Coupled with an Absorption Refrigeration Cycle. *J. Therm. Sci.* **2020**, *29*, 1036–1052. [[CrossRef](#)]
34. Zhang, Y.Q.; He, Y.N.; Wang, Y.L.; Wu, X.H.; Jia, M.Z.; Gong, Y. Experimental investigation of the performance of an R1270/CO₂ cascade refrigerant system. *Int. J. Refrig.* **2020**, *114*, 175–180. [[CrossRef](#)]
35. Shen, J. *Design of Refrigeration Units*; Machinery Industry Press: New York, NY, USA, 2011.
36. Guo, Y.J.; Xie, J.; Zhu, S.X.; Wang, J.F. Techno-economic analysis of two-staged compression and cascade compression refrigeration system. *Chem. Ind. Eng. Process.* **2015**, *34*, 3194–3201.